The Surface Properties of Clay Minerals Modified by Intensive Dry Milling – Revisited

Neda Vdović[a], Irena Jurina[a], Srečo D. Škapin[b], and Ivan Sondi*[a]

[a]Center for Marine and Environmental Research, *Ruđer Bošković* Institute, Bijenička cesta 54, 10000 Zagreb, Croatia.
[b]Advanced Materials Department, *Jožef Stefan* Institute, Jamova 39, 1000 Ljubljana, Slovenia

*corresponding author

Abstract

The present study broadened the research on the effect of the intensive physical disintegration of clay minerals (kaolinite and “Otay” montmorillonite) and mica (ripidolite), carried out by high-energy ball milling (HEBM), on their surface physico-chemical characteristics, i.e., the specific surface area (SSA), the cation exchange capacity (CEC), and the electrokinetic properties. The mechanical disintegration of clay minerals occurred in two consecutive processes. Significant changes of the size, morphology and structure were followed by the change of the physico-chemical properties. The decrease of the particle size of the clay minerals resulted in significant increases in the SSA and CEC values, and in the exposure of new, amphoteric surfaces, significantly changing the electrophoretic mobility (EPM). Prolonged milling produced amorphous alumina-silicate aggregates. These solids exhibited the same morphological properties, SSA and CEC, despite the fact that they were formed from initially different clay minerals. In contrast, the electrophoretic mobility of these samples was significantly changed, exemplifying the significance of the initial chemical composition and the formation of different types of surface structures on the physico-chemical processes at amorphous solid-surface–liquid interfaces.

Keywords: ball-milling, electrokinetics, kaolinite, montmorillonite, ripidolite, surface characteristics

1. Introduction

Many applications of clay minerals depend on their particle size and surface properties (Addai-Mensah and Ralston, 2005; Derkowski *et al*., 2006; Marwa *et al*., 2009). Small-sized clay mineral particles exhibit the physico-chemical characteristics of colloidal particles and are suitable for numerous catalytic, ceramic, and engineering applications, owing their applicability to a large specific surface area and surface reactivity. Biogeochemical processes in soils and aquatic sediments are mainly governed by physico-chemical reactions at the surface of their colloidal constituents, particularly clay minerals (Sondi *et al*., 1994, 2008). These processes are governed by their electrokinetic properties, large specific surface area and high cation exchange capacity (Sondi and Pravdić, 1998; Churchman at al., 2006).

The surface and bulk properties of minerals can be modified by physical weathering, reducing the particle size. Weathering occurs continuously in nature and changes size, morphology, and bulk properties of the mineral components, and form new mineral phases (Brown at al., 1978; Dubroeucq *et al*., 1998; Ndayiragije and Delvaux, 2003). Weathering in nature involves long time-scale processes in geographically extended areas, which prevents the monitoring of these processes *in situ*. The practical way to avoid these impasses is experimental laboratory work, where the effect of size reduction on changes of the surface and bulk properties can be monitored over short time periods.

Lately, formation and characterization of micron and submicron-size clay minerals, obtained by the ultrasound treatment of mica-group minerals such as vermiculite (Perez-Maqueda *et al*., 2001) and muscovite and biotite (Perez- Maqueda *et al*., 2003) have been studied. The literature also abounds with studies of the influence of mechanical processes on the structural and physico-chemical properties of a variety of clay minerals (Suray *et al*., 1997; Baudet *et al*., 1999; Sanchez-Soto *et al*., 2000; Frost *et al*., 2001; Franco *et al*., 2004; Dellisanti and Valdré, 2005; Hrachová *et al*., 2007; Vertuccio *et al*., 2009). The rapid development of the new, composite clay-based materials has advanced the research and processing of fine-milling and reinforcing methods. Recently, high-energy ball milling (HEBM) has been recognized as an efficient method for particle size comminution, structural changes and the optimization of the powder properties (Morrell and Man, 1997; Sondi *et al*., 1997; Mio *et al*., 2004; Wei and Craig, 2009).

This study aims to investigate the effects of particle size reduction and the resulting structural changes, induced by the HEBM technique, on the electrokinetic and surface properties of different clay minerals. It assesses the degree to which short-term laboratory experiments are significant for studies of the particle size diminution processes of clay and mica minerals in nature. It is also intended to contribute to the understanding of the mechanism of the formation of amorphous secondary aluminosilicate colloidal solids in natural environments. Finally, this study supports the development of new methods capable of generating novel sub-micron size clay mineral particles with stringent control of their structural, morphological, and colloidal properties that are required for specific needs in material science.

2. Experimental

2.1. Materials

The minerals selected for these investigations were montmorillonite (2:1 type), kaolinite (1:1 type), and chlorite-ripidolite (2:1:1 type). These solids were chosen on account of the differences in their structural properties and because of their common occurrence in natural soils and sediments. Montmorillonite type "Otay" (SBCa-1, California) and chlorite-ripidolite (CCa-1, Flagstaff Hill, CA) were obtained as standard reference minerals from the Clay Minerals Society, Source Clay Minerals Repository, University of Missouri, Columbia, MO. A well-crystallized kaolinite was purchased from the Aldrich Chemical Company.

2.2. Methods

The physical disintegration of clay mineral solids was performed by high-energy ball milling (HEBM) using a planetary ball-mill Pulverisette 7 (Fritsch, Germany). An amount of 300 mg of solid was placed in an agate vessel containing 10 tungsten carbide balls (Φ =10 mm) and the vessel was rotated at 3000 r.p.m. for predetermined times (t_m). The obtained powders were then analyzed using the following techniques:

The structural changes of the clay mineral solids during the milling process were determined by X-ray powder diffraction (XRD), using a D4 Endeavor, Bruker AXS instrument. The structural changes were examined with a high-resolution transmission electron microscope (HRTEM, Philips, CM-20) and a scanning electron microscope (FE-SEM SUPRA 35VP, Carl Zeiss), equipped with an energy-dispersive spectrometer (EDXS, Inca 400, Oxford Instruments).

The specific surface area (SSA) measurements were made using the single-point nitrogen-adsorption technique, with a Micromeritics FlowSorb II 2300 instrument. The cation exchange capacity (CEC) was determined by using ammonia exchange and an ammonia-specific electrode (Busenberg and Clemency, 1973).

The electrokinetic mobility (EPM) of the clay mineral particles was measured as a function of pH in a $1x10^{-3}$ mol dm^{-3} aqueous NaCl solution with a ZetaPals instrument (Brookhaven Instruments, USA). Approximately 20 mg of each sample were dispersed in 100 ml of an inert electrolyte and left for a few hours at a constant temperature of 25^{0}C to reach equilibrium. The EPM of the dispersed particles was then measured. The initial dispersion was titrated with an acid or base, and the EPM was measured after each pH change at a constant temperature of 25^{o}C.

Next to the EPM, shown in Figs. 6-9, the values of the zeta-potentials, calculated by the Helmholtz – Smoluchowski equation with the Henry extension, are quoted. Expressing the data in terms of zeta-potentials gives a more comprehensible insight into the results obtained in this study.

The instrument was tested prior to measurements using standard calibrating polysterene latex, supplied by the manufacturer.

3. Results

The XRD patterns of the kaolinite (Fig. 1A), ripidolite (Fig. 1B) and Otay-montmorillonite (Fig. 1C) after different times of the HEBM treatment were displayed in Fig. 1. Rapid structural changes during the milling process, showing a loss of the crystalline phase, occurred in all the investigated solids. This was evidenced by a progressive decrease of the XRD reflection intensities. In addition, the broadening of the XRD reflections (Fig. 1, spectra b) indicated that, along with structural changes, a reduction in particle size occurred. With prolonged milling (256 min.) these clay minerals were transformed into fully amorphous solids.

The original kaolinite was characterized by plate-like pseudohexagonal particles (Fig. 2A). Milling during 16 min. decreased the particle size, and a polydispersed powder of irregularly shaped particles was formed (Fig. 2B). Prolonged milling caused discernible differences in the size and shape of the particles, *i.e.*, larger particle aggregates composed of smaller nanoparticles were formed (Fig. 2C, D). The particles were amorphous (Fig. 1A-C, spectra c). The same observations were made during milling of montmorillonite and ripidolite.

The (00l) planes of the original ripidolite particles with undisturbed lattice fringes (basal repeating unit) of 1.4 nm are shown in Fig. 3A. Milling caused a significant deformation, bending and breaking of the basal 00l planes (Fig. 3B). With prolonged milling, all the structural features, typical for clay minerals, disappeared (Fig. 3C).

The initial specific surface areas of kaolinite, chlorite and montmorillonite were 12, 2.4 and 71 m^2g^{-1}, and were increased with increasing milling time (Fig. 4). The maximum specific surface area was obtained after approximately 16 min. of milling (39 m^2g^{-1} for kaolinite, 20 m^2g^{-1} for chlorite and 99 m^2g^{-1} for montmorillonite). Prolonged milling decreased the SSA in all three cases. A similar trend was observed for the CEC (Fig. 5). The initial CEC values for the kaolinite, chlorite and montmorillonite were 12, 1.5 and 142 $cmol_c$ kg^{-1}, respectively, and they reached their maxima (26, 15 and 175 $cmol_c$ kg^{-1}) after 16 minutes of milling. Further treatment caused a significant decrease of the CEC values, reaching values of approximately 10 $cmol_c$ kg^{-1}.

The EPM of all three raw mineral samples was negative across the whole investigated pH range (Fig 6-8). In the range of pH = 2–8, montmorillonite retained an almost constant negative ζ-potential (ζ = -30 to -35 mV), while the ζ-potential values of kaolinite and chlorite, in the same pH range, were between -20 and -55 mV and between -5 and -30 mV, respectively.

The ζ-potential of the montmorillonite, after 16 minutes of milling, assumed a less-negative value at a low pH (ζ = -10 mV). Kaolinite and chlorite reached positive values at low pH. The isoelectric point (IEP) of kaolinite was recorded at pH ≈ 3, of chlorite at pH ≈ 6.5.

Prolonged milling (256 minutes) caused an additional change in the electrophoretic behavior of these minerals. The ζ-potential of the montmorillonite approached the IEP in acidic conditions (pH = 2) and a very high negative value of ζ = -55 mV at higher pH. In the case of the kaolinite and chlorite, the ζ-potential was additionally shifted towards more positive values; the IEP of kaolinite was reached at pH = 4.5, and that of chlorite at pH = 7.2.

4. Discussion

The results obtained in this study showed that the intensive physical disintegration of the clay minerals by high energy ball milling consisted of two processes, *i.e.*, particle size reduction and morphological and structural changes, accompanied by changes of the surface properties.

There are several aspects concerning these two processes that should be addressed. The first process, which applies to all the investigated solids during the early stages of the HEBM treatment, refers to the intensive decrease of the initial particle size, associated with morphological changes and the formation of a polydispersed powder with a markedly irregular particle shape. Similar to our previous work, the fracturing and size reduction of the clay mineral particles during this process occur in two steps: (1) an initial cleavage along the basal planes and the exposure of new basal planes, and (2) a break up of the particles in perpendicular to the basal plane (Sondi *et al*., 1997). As a consequence, the SSA and the CEC increase.

On prolonged milling, a substantial structural deformation and alteration occurs, followed by the transformation of the crystalline structure into an amorphous phase; as recently described by Dellisanti and Valdré (2005) for bentonite, and by Makó *et al*. (2001) and Sanchez-Soto et al., (2000) for kaolinite. The latter study has shown that milling produced vigorous structural changes along the c axis, resulting in disorder and degradation of the crystal structure of the kaolinite and the formation of an amorphous solid. This is reflected in the XRD line broadening, increases in the main lattice strains, and a reduction of the reflection intensities. The same was found for the clay mineral particles investigated in this study.

A further, somewhat unique, observation was that the finally obtained amorphous solids showed the same morphological, SSA and CEC properties, despite the fact that they were formed from initially different clay minerals in terms of their structure, surface and chemical properties. This implies that the intensive mechanical treatment of different clay minerals causes the formation of amorphous aluminosilicates with similar structural, morphological and SSA, and CEC properties.

The structural changes of the clay minerals obtained during the HEBM process were also reflected in their electrokinetic properties. As expected, all the original clay minerals did not have IEPs in the pH range 2 to 9. However, kaolinite and ripidolite showed a distinct decrease in the values of the negative potentials with increasing pH. This is in agreement with our previous studies, showing that the electrokinetic properties of raw and purified clay minerals vary depending on their structural properties, mostly on the presence and the proportion of pH-dependent amphoteric edge surfaces. In the case of montmorillonite, that ratio was much more in favour of the less-reactive siloxane basal surface, reaching approximately 99% of the total external surface area (Greene-Kelly, 1964) and characterized by the constant pH-independent charge (Miller and Low, 1990, Thomas *et al*., 1999). The data for raw kaolinite and chlorite demonstrated the much stronger pH-dependence of the ζ-potential, indicating a higher proportion of amphoteric surface sites (edges) compared to that of montmorillonite (Zhou and Gunter, 1992, Tombácz and Szekeres, 2004, 2006).

The electrophoretic mobility of all three minerals assumed less negative values after milling. The most pronounced changes were detected in the case of kaolinite and chlorite. At low pH even positive values were reached confirming the previous observation of the critical role of disintegration on the creation of new “edges”, their increasing contribution to the total surface area and the change of the electrokinetic properties (Sondi *et al*., 1997). What was previously not appreciated is the fact that, in comparison with the SSA and CEC values, the obtained amorphous solids of different types of clay minerals did not show similar electrokinetic characteristics. The obvious question is: how did these differences occur?

It seems that the changes in the surface characteristics (SSA and CEC) of the clay minerals during physical weathering are governed exclusively by their size diminution and the morphological and structural changes. The kinetics of these processes should be the same for all three types of solids, and would consequently, for their finally obtained amorphous solids, result in the same SSA and CEC values. In contrast, the electrophoretic mobility of these samples showed different aspects, elucidating the significance of the chemical composition of the source materials. Milling led to new types of surface structures indicated by the electrokinetic properties. Thus, this study supports the concept of the mechanochemical formation of new aluminosilicate materials with a surface structure very different from that of the untreated, or, slightly structurally changed materials (Frost *et al*., 2001). The electrokinetic properties of the obtained solids are determined by the dynamic exchange due to adsorption, ion-pair formation, surface complexation, precipitation, and dissolution processes (Tombácz, 2002).

The present work approximates the processes of the physical weathering of clay mineral particles in natural environments and clarifies some of the complex phenomena in the surface-charge formation of the structurally and chemically different minerals obtained by physical disintegration. The size diminution caused by the fragmentation of clay mineral constituents opens new surfaces for the reactions with the surrounding medium/solution and renders the mineral particles more reactive in biogeochemical processes. Combined with chemical weathering, these processes may lead to the formation of new, mineral phases, *e.g*. allophane (Brown *et al*., 1978), even smaller in size and amorphous in structure. At the same time, this study assists in the development of new methods capable of generating sub-micron-sized solids with stringent control of their morphological and colloidal properties that are required for specific cases in materials science.

Acknowledgement:

This work was supported by the Ministry of Science, Education and Sports of the Republic of Croatia (Grants 098-0982934-2742, 119-0000000-1158), and by the Ministry of Higher Education, Science and Technology of the Republic of Slovenia (Grant P2-0091-0106).

References:

Addai-Mensah, J., Ralston, J., 2005. Investigation of the role of interfacial chemistry on particle interactions, sedimentation and electroosmotic dewatering of model kaolinite dispersions. Powder Technology 160, 35-39.

Baudet, G., Perrotel, V., Seron, A., Stellatelli, M., 1999. Two dimensions comminution of kaolinite clay particles. Powder Technology 105, 125-134.

Brown, G., Newman, A.C.D., Rayner, J.H., Weir, A.H., 1978. The structure and chemistry of soil clay minerals. In: D.J. Greenland, M.H.B. Hayes (Eds.), The chemistry of soil constituents. John Wiley and Sons, Chichester, pp. 29-178.

Busenberg, E., Clemency, C.V., 1973. Determination of the cation exchange capacity of clays and soils using an ammonia electrode. Clays and Clay Minerals 21, 213-217.

Churchman, G.J., Gates, W.P., Theng, B.K.G., Yuan, G., 2006. Clays and clay minerals for pollution control. In: F. Bergaya, B.K.G. Theng, G. Lagaly (Eds.), Handbook of Clay science. Elsevier, Amsterdam, pp. 625-675.

Dellisanti, F., Valdré, G., 2005. Study of structural properties of ion treated and mechanically deformed commercial bentonite. Applied Clay Science 28, 233-244.

Derkowski, A., Franus, W., Beran, E., Czimerova, A., 2006. Properties and potential applications of zeolitic materials produced from fly ash using simple method of synthesis. Powder Technology 166, 47-54.

Dubroeucq, D., Geissert, D., Quantin, P., 1998. Weathering and soil forming processes under semi-arid conditions in two Mexican volcanic ash soils. Geoderma 86, 99-122.

Franco, F., Pérez-Maqueda, L.A., Pérez-Rodríguez, J.L., 2004. Influence of the particle-size reduction by ultrasound treatment on the dehydroxylation process of kaolinites. Journal of Thermal Analysis and Calorimetry 78, 1043-1055.

Frost, R.L., Makó, E., Kristóf, J., Horváth, E., Kloprogge, J.T., 2001. Modification of kaolinite surfaces by mechanochemical treatment. Langmuir 17, 4731-4738.

Greene-Kelly, R., 1964. The specific surface areas of montmorillonites. Clay Minerals Bulletin 5, 392-400.

Hrachová, J., Madejová, J., Billik, P., Komadel, P., Fajnor, V.Š., 2007. Dry grinding of Ca and octadecyltrimethylammonium montmorillonite. Journal of Colloid and Interface Science 316, 589-595.

Makó, E., Frost, R.L., Kristóf, J., Horváth, E., 2001. The effect of quartz content on the mechanochemical activation of kaolinite. Journal of Colloid and Interface Science 244, 359-364.

Marwa, E.M.M., Meharg, A.A., Rice, C.M., 2009. The effect of heating temperature on the properties of vermiculites from Tanzania with respect to potential agronomic applications. Applied Clay Science 43, 376-382.

Miller, S.E., Low, P.F., 1990. Characterization of the electrical double layer of montmorillonite. Langmuir 6, 572-578.

Mio, H., Kano, J., Saito, F., Kaneko, K., 2004. Optimum revolution and rotational directions and their speeds in planetary ball milling. International Journal of Mineral Processing 74S, S85-S92.

Morrell, S., Man, Y.T., 1997. Using modelling and simulation for the design of full scale ball mill circuits. Minerals Engineering 10, 1311-1327.

Ndayiragije, S., Delvaux, B., 2003. Coexistence of allophane, gibbsite, kaolinite and hydroxy-Al-interlayered 2:1 clay minerals in a perudic Andosol. Geoderma 117, 203-214.

Pérez-Maqueda, L.A., Caneo, O.B., Poyato, J., Pérez-Rodríguez, J.L., 2001. Preparation and characterization of micron and submicron-sized vermiculite. Physics and Chemistry of Minerals 28, 61-66.

Pérez-Maqueda, L.A., Franco, F., Avilés, M.A., Poyato, J., Pérez-Rodríguez, J.L., 2003. Effect of sonication on particle-size distribution in natural muscovite and biotite. Clays and Clay Minerals 51, 701-708.

Sanchez-Soto, P.J., de Haro, M.D.J., Pérez-Maqueda, L.A., Varona, I., Pérez-Rodríguez, J.L, 2000. Effects of dry grinding on the structural changes of kaolinite powders. Journal of the American Ceramic Society 83,1649-1657.

Sondi, I., Juračić, M., Prohić, E., Pravdić, V., 1994. Particulates and the environmental capacity for trace metals. A small river as a model for a land-sea transfer system: The Raša River estuary. Science of Total Environment 155, 173-185.

Sondi, I., Stubičar, M., Pravdić, V., 1997. Surface properties of ripidolite and beidellite clays modified by high-energy ball milling. Colloids and Surfaces A: Physicochemical and Engineering Aspects 127, 141-149.

Sondi, I., Pravdić, V., 1998. The colloid and surface chemistry of clays in natural waters. Croatica Chemica Acta 181, 463-469.

Sondi, I., Lojen, S., Juračić, M., Prohić, E., 2008. Mechanisms of land-sea interactions – the distribution of metals and sedimentary organic matter in sediments of a river-dominated Mediterranean karstic estuary. Estuarine, Coastal and Shelf Science 80, 12-20.

Suraj, G., Iyer, C.S.P., Rugmini, S., Lalithambika, M., 1997. The effect of micronization on kaolinites and their sorption behaviour. Applied Clay Science 12, 111-130.

Thomas, F., Michot, L.J., Vantelon, D., Montargès, E., Prélot, B., Cruchaudet, M., Delon, J.F., 1999. Layer charge and electrophoretic mobility of smectites. Colloids and Surfaces A: Physicochemical and Engineering Aspects 159, 351-358.

Tombácz, E., 2002. Adsorption from electrolyte solutions. In: J. Tóth (Ed.), Adsorption: Theory modeling and analysis. Marcel Dekker, New York, pp. 29-178.

Tombácz, E., Szekeres, M., 2004. Colloidal behavior of aqueous montmorillonite suspensions: The specific role of pH in the presence of indifferent electrolytes. Applied Clay Science 27, 75-94.

Tombácz, E., Szekeres, M., 2006. Surface charge heterogeneity of kaolinite in aqueous suspension in comparison with montmorillonite. Applied Clay Science 34, 105-124.

Vertuccio, L., Gorrasi, G., Sorrentino, A., Vittoria, V., 2009. Nano clay reinforced PCL/starch blends obtained by high energy ball milling. Carbohydrate Polymers 75, 172-179.

Wei, D., Craig, I.K., 2009. Grinding mill circuits: A survey of control and economic concerns. International Journal of Mineral Processing 90, 56-66.

Zhou, Z., Gunter, W.D., 1992. The nature of the surface charge of kaolinite. Clays and Clay Minerals 40, 365-368.

Figure Caption

1. XRD patterns of kaolinite (A), ripidolite (B) and montmorillonite (C) after the HEBM for various times: (a) 0, (b) 16 and (c) 256 min.
2. SEM photomicrographs of kaolinite particles after HEBM for (A) 0, (B) 16 and (C, D) 256 min.
3. HRTEM photomicrographs of ripidolite particles after HEBM for (A) 0, (B) 16 and (C) 256 min.
4. Specific surface area (SSA) after HEBM for various times.
5. Cation exchange capacity (CEC) after HEBM for various times.
6. Electrophoretic mobility and zeta-potential of kaolinite particles after HEBM, dispersed in a $1x10^{-3}$mol dm^{-3} NaCl solution, as a function of pH.
7. Electrophoretic mobility and zeta-potential of ripidolite solids particles after HEBM, dispersed in a $1x10^{-3}$mol dm^{-3} NaCl solution, as a function of pH.
8. Electrophoretic mobility and zeta-potential of Otay montmorillonite particles after HEBM, dispersed in a $1x10^{-3}$mol dm^{-3} NaCl solution, as a function of pH.

Figure 1.

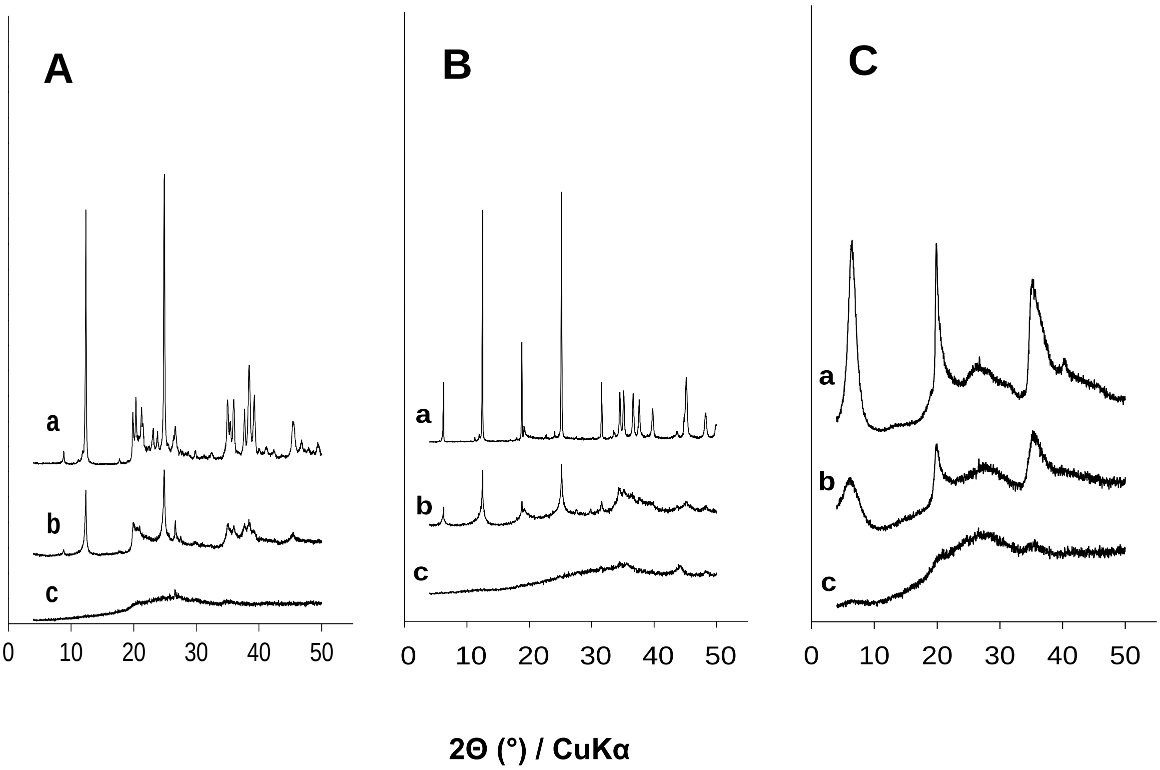
A
a
b
c
0
10
20
30
40
50
B
a
b
c
0
10
20
30
40
50
C
a
b
c
0
10
20
30
40
50
2Θ (°) / CuKα

Figure 2.

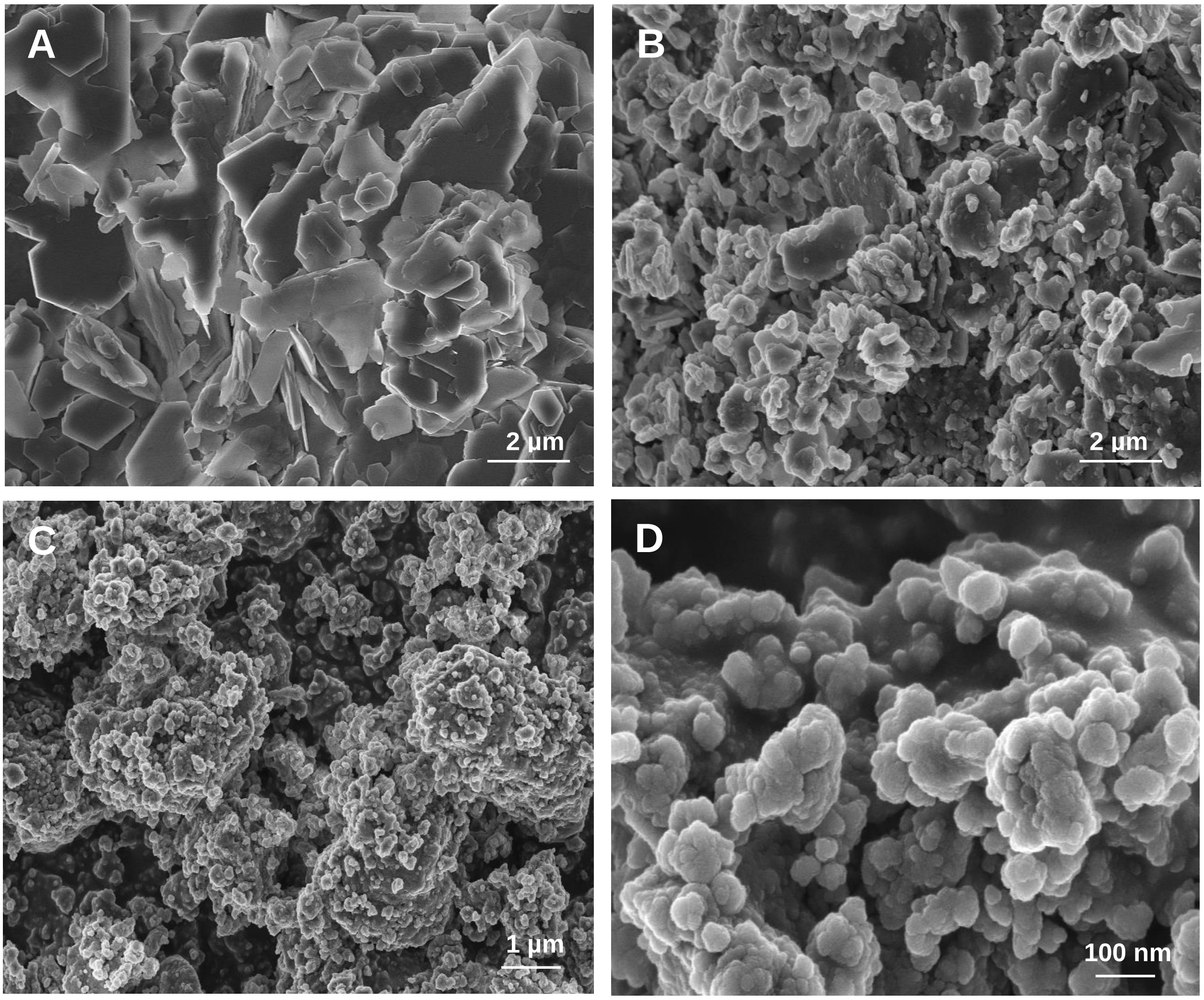

Figure 3.

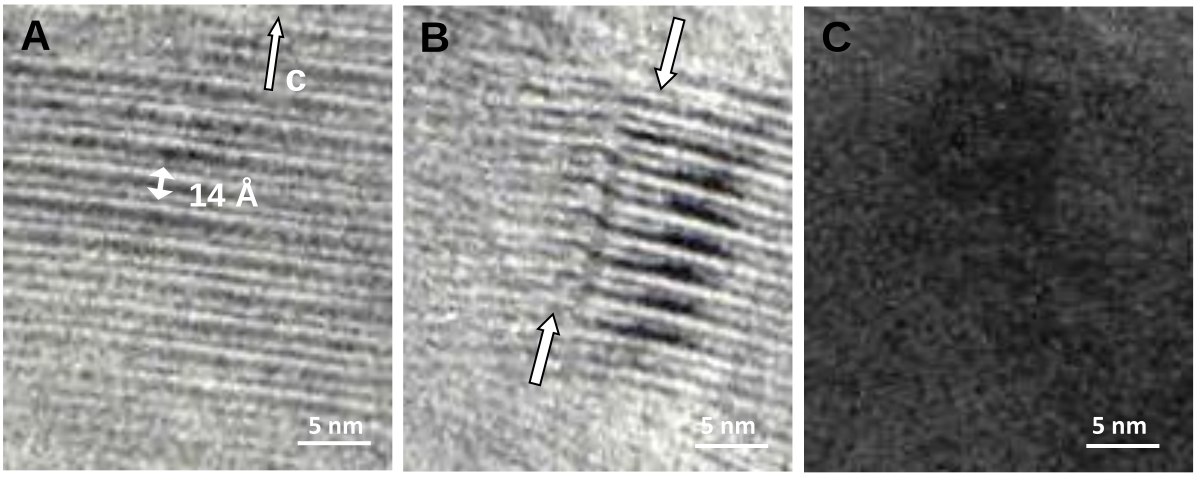

Figure 4.

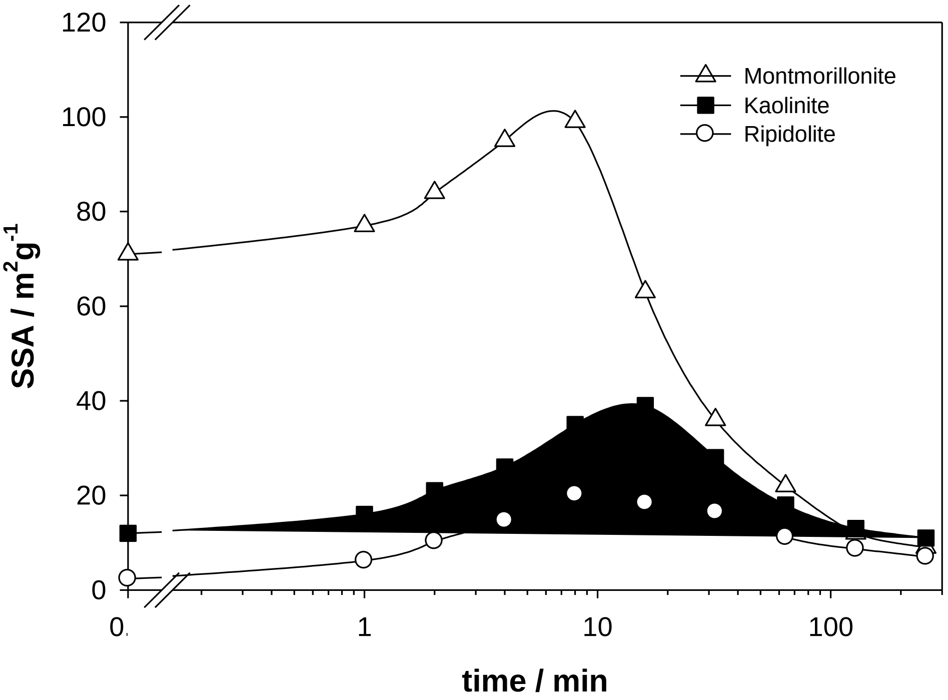
120
100
80
60
40
20
0
SSA / m^2g^{-1}
0.
1
10
100
time / min
Montmorillonite
Kaolinite
Ripidolite

Figure 5

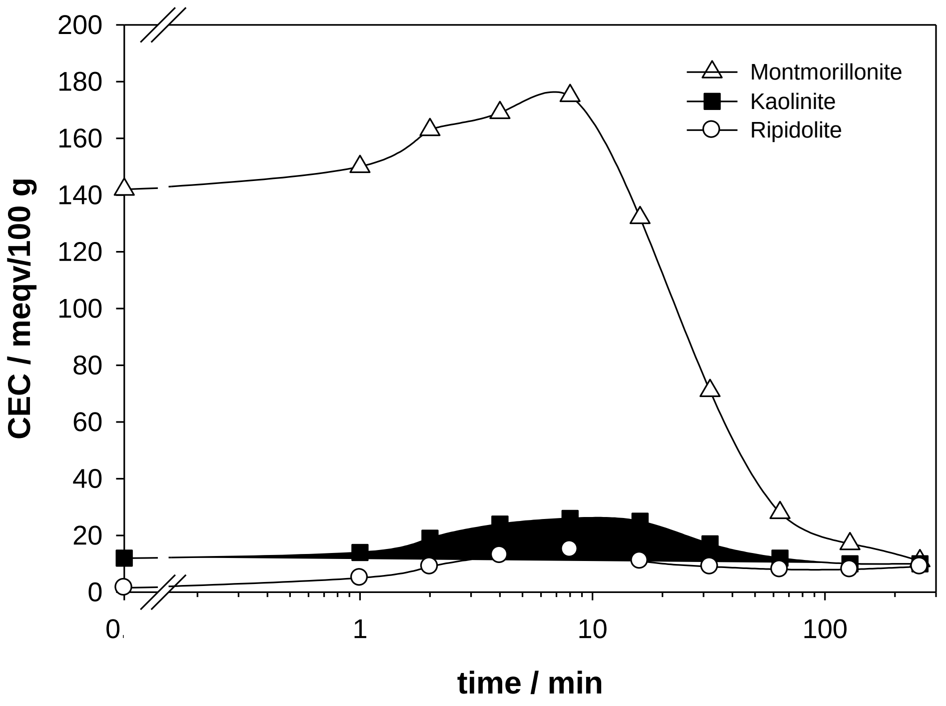
200
180
160
140
120
100
80
60
40
20
0
CEC / meqv/100 g
0.
1
10
100
time / min
Montmorillonite
Kaolinite
Ripidolite

Figure 6

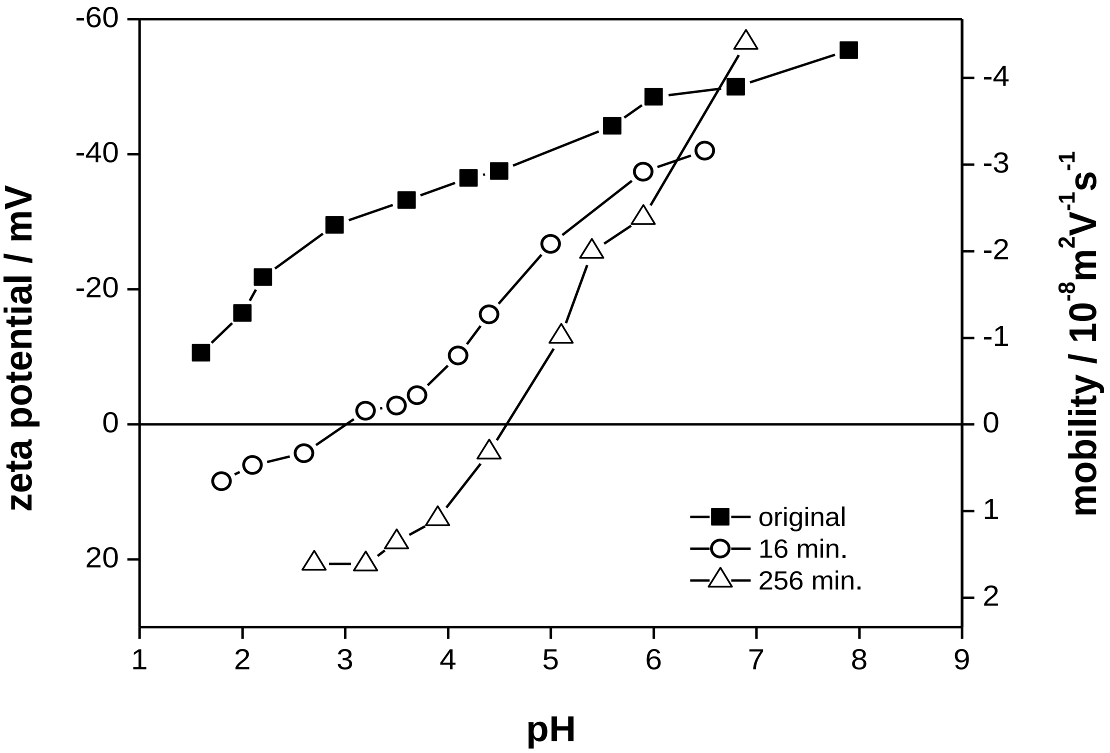
-60
-40
-20
0
20
zeta potential / mV
-4
-3
-2
-1
0
1
2
mobility / 10^{-8} $m^2V^{-1}s^{-1}$
1
2
3
4
5
6
7
8
9
pH
original
16 min.
256 min.

Figure 7

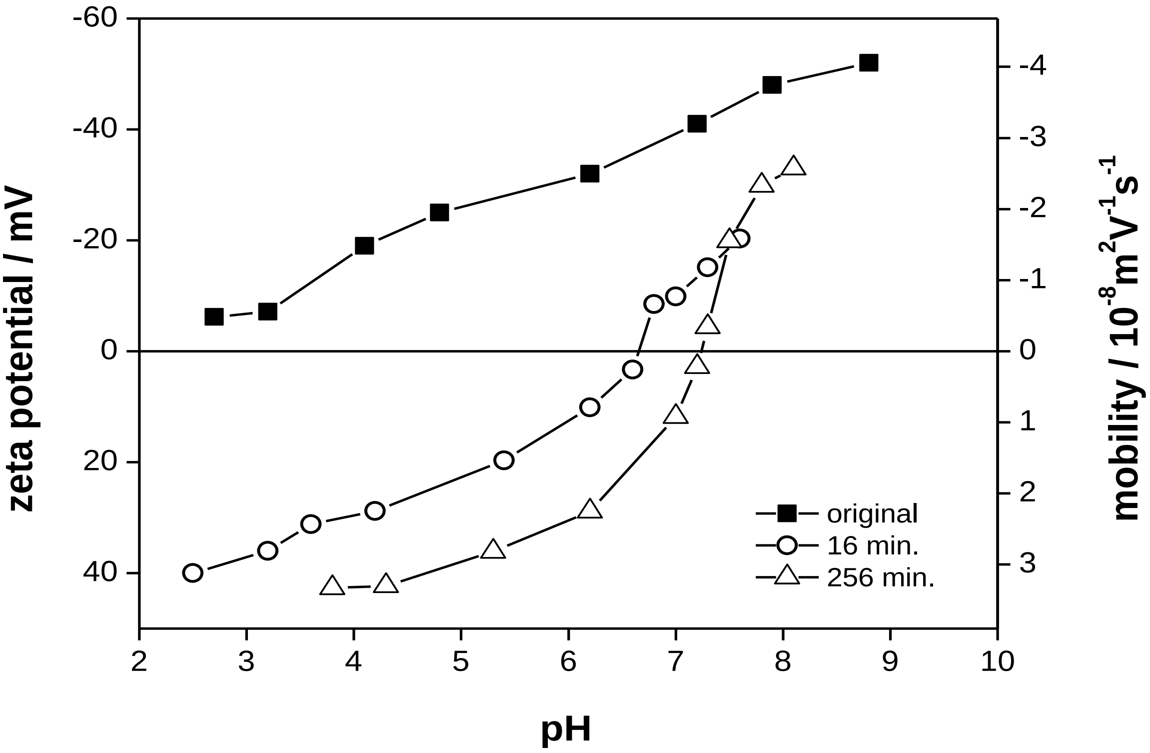
-60
-40
-20
0
20
40
-4
-3
-2
-1
0
1
2
3
zeta potential / mV
mobility / $10^{-8} m^2V^{-1}s^{-1}$
2
3
4
5
6
7
8
9
10
pH
original
16 min.
256 min.

Figure 8

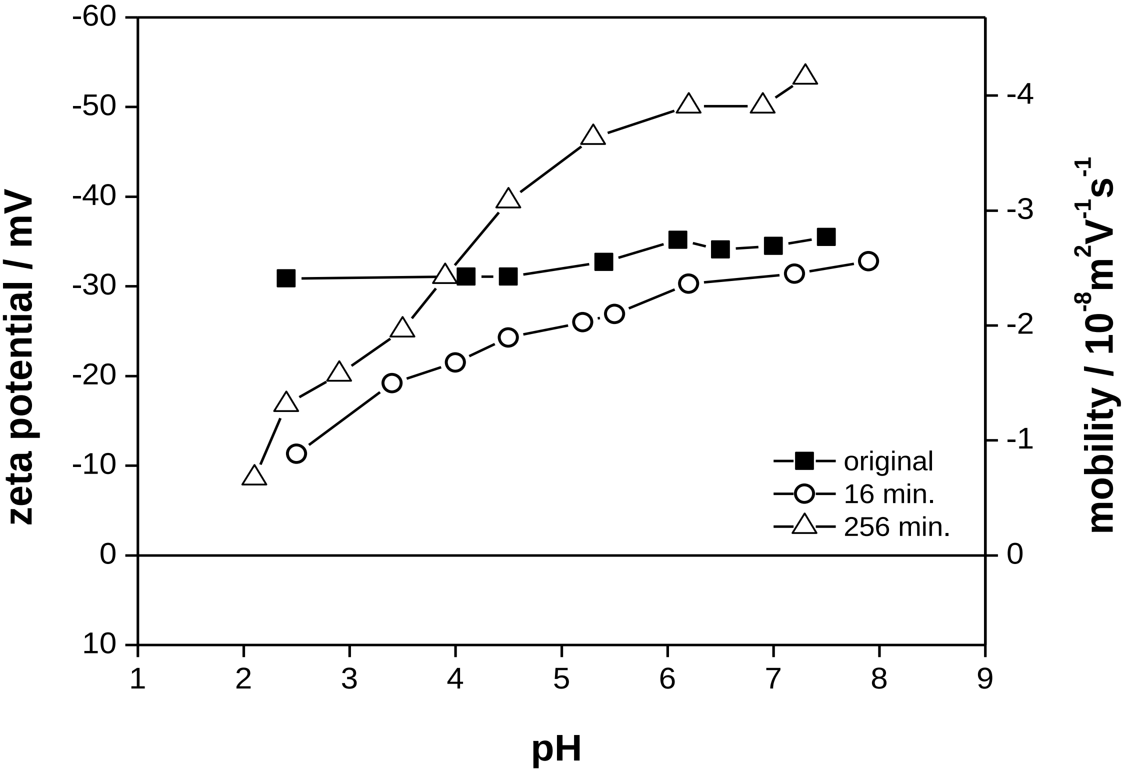
zeta potential / mV
-60
-50
-40
-30
-20
-10
0
10
mobility / $10^{-8}m^2V^{-1}s^{-1}$
-4
-3
-2
-1
0
1
2
3
4
5
6
7
8
9
pH
original
16 min.
256 min.